

# A 40,000 year unchanging seismic regime in the Dead Sea rift

Z.B. Begin\* Geological Survey of Israel, 30 Malche Yisrael Street, Jerusalem 95501, Israel

D.M. Steinberg Department of Statistics and Operations Research, Tel Aviv University, Levanon Street, Tel Aviv 69778, Israel

G.A. Ichinose URS Group International Inc., 566 El Dorado, Pasadena, California 912101-2560, USA

S. Marco Department of Geophysics and Planetary Sciences, Tel Aviv University, Levanon Street, Tel Aviv 69978, Israel

## ABSTRACT

We studied breccia beds in lacustrine sediments within the active Dead Sea basin. The beds were deformed by  $M > 5.5$  earthquakes during the past 60 k.y. Our new analysis considers both the thickness of breccia beds and the lithology of beds directly overlying them in order to identify 11  $M > 7$  earthquakes that originated within the Dead Sea pull-apart between 54 and 16 ka. The resulting time series is a unique long record of earthquakes in a well-constrained segment of a fault system in which the time interval between consecutive earthquakes increased from hundreds of years to a background recurrence interval of  $\sim 11$  k.y. since ca. 40 ka. Since this recurrence interval is similar to the  $M \geq 7.2$  recurrence interval in the Dead Sea basin, as extrapolated from present seismicity, we suggest that the present seismic regime in the Dead Sea basin, as reflected in its magnitude-frequency relation as well as in its deficiency in seismic moment, has been stationary for the past  $\sim 40$  k.y. Since the increasing interval between consecutive earthquakes in the studied segment of the Dead Sea fault is time-logarithmic, it may be a result of healing of the brittle crust as well as a diminishing strain rate following the first strong earthquake in the sequence.

**Keywords:** paleoseismicity, tsunami, relaxation, Dead Sea rift.

## INTRODUCTION

We studied a paleoseismic record within the active Dead Sea pull-apart (Garfunkel, 1981). The record was extracted from the 70–14 ka lacustrine sediments of the Lisan Formation, in which  $\sim 30$  breccia beds were interpreted as having been induced by  $M > 5.5$  earthquakes (Marco and Agnon, 1995; Marco, 1996; Marco et al., 1996). This interpretation was further substantiated when ages of similar brecciated beds in the Dead Sea deposits were found to match historical earthquakes (Kentor et al., 2001; Migowski et al., 2004). However, no distinction was previously made between moderate and strong earthquakes in the Lisan record, and their epicentral distance was not well constrained. This study is an attempt to identify the stronger earthquakes in the Lisan paleoseismic record and to constrain the location of their source.

## SETTING

We reexamined two 40-m-thick sections of the Lisan Formation, PZ1 (coordinates 18450/05599, Israel old grid) and PZ2 (coordinates 18500/05800) (Marco, 1996; Marco et al., 1996), which are 2 km apart (Fig. 1). The PZ1 section is well dated by 22 U-Th age determinations (Schramm et al., 2000; Haase-Schramm et al., 2004), which allows a good estimate ( $\pm 0.8$  k.y.) for the ages of its breccia beds for the period 60–14 ka, with the excep-

tion of a sedimentation hiatus at 49–44 ka during a stage of low lake level (Fig. 2). The two sections are composed mainly of alternating laminae of authigenic aragonite and detrital silt-clay ( $\sim 55\%$  of the beds), which represent the normal annual deposition in paleolake Lisan. The rest of the sections comprise detrital beds, mainly of sand size (36% and 19% in PZ2 and PZ1, respectively), plus alternating laminae of authigenic gypsum and sand-size detritus (4% and 25% in PZ2 and PZ1, respectively) and authigenic massive gypsum (3% of the beds). The higher percentage of detritus in PZ2 reflects its deposition in closer proximity to an alluvial fan (Machlus et al., 2000). For each breccia bed in the two sections, we recorded the lithology of beds below and above it. (See GSA Data Repository Tables DRA–DRC.<sup>1</sup>)

## RESULTS

We found that in both the PZ1 and PZ2 sections the distribution of the lithology of beds below and above the brecciated beds is not symmetrical (Tables DRB, DRC; see footnote 1). In the PZ2 section there is a highly significant preference for brecciated beds overlain by detritus (BD), whereas in the PZ1 sec-

tion there is a weak preference for brecciated beds overlain by laminated gypsum and detritus (BGD) or by detritus. The importance of BGD and BD couplets is further emphasized by another independent observation that brecciated beds in these couplets are significantly thicker than brecciated beds that are overlain by aragonite laminae. The thicker the bed, the higher the probability that it is overlain by laminated gypsum and detritus or by detritus (Fig. 3; Fig. DRD [see footnote 1]).

We propose that the common factor explaining these two independent associations is strong earthquakes. On one hand, accepting that the brecciated beds in the Lisan Formation were formed by earthquake-induced fluidization or liquefaction (Marco and Agnon, 1995; Marco, 1996; Marco et al., 1996; Kentor et al., 2001; Migowski et al., 2004), we assume that thicker brecciated beds indicate higher earthquake intensity. This is reasonable in light of the correlation between the liquefaction severity index and earthquake magnitude (Youd and Perkins, 1987), and because stronger earthquakes that last longer may cause more stress cycles at a site (Seed and Idriss, 1982), which in turn may bring about higher pore pressure within the sediment. On the other hand, the formation of gypsum ( $\text{CaSO}_4 \cdot 2\text{H}_2\text{O}$ ) in paleolake Lisan was attributed to mixing of its sulfate-rich upper water layer and the calcium-rich lower water layer (Stein et al., 1997). It was previously suggested that such mixing took place due to climatic change toward dryness (Stein et al., 1997), but we propose an additional cause for the mixing of the Lake Lisan water column: high waves (tsunamis and seiches) following strong earthquakes. We assume that some of the strong earthquakes that brought about the formation of brecciated beds were also associated with faulting that generated high seiches, forming gypsum that was deposited directly above the brecciated beds. Hence, whereas some gypsum beds in the Lisan Formation were formed with no association to earthquakes, BGD couplets in the Lisan Formation may be considered to be seismites representing strong earthquakes. This model is supported by the observations regarding detritus beds overlying brecciated beds in the PZ2 section, since the formation of detrital beds above tsunamites, resulting from tsuna-

\*Corresponding author e-mail: begin\_bz@mail.gsi.gov.il.

<sup>1</sup>GSA Data Repository item 2005045, Tables DRA–DRC, detailed data for the PZ1 and PZ2 brecciated beds, and Figure DRD, logistic function, are available online at [www.geosociety.org/pubs/ft2005.htm](http://www.geosociety.org/pubs/ft2005.htm), or on request from [editing@geosociety.org](mailto:editing@geosociety.org) or Documents Secretary, GSA, P.O. Box 9140, Boulder, CO 80301–9140, USA.

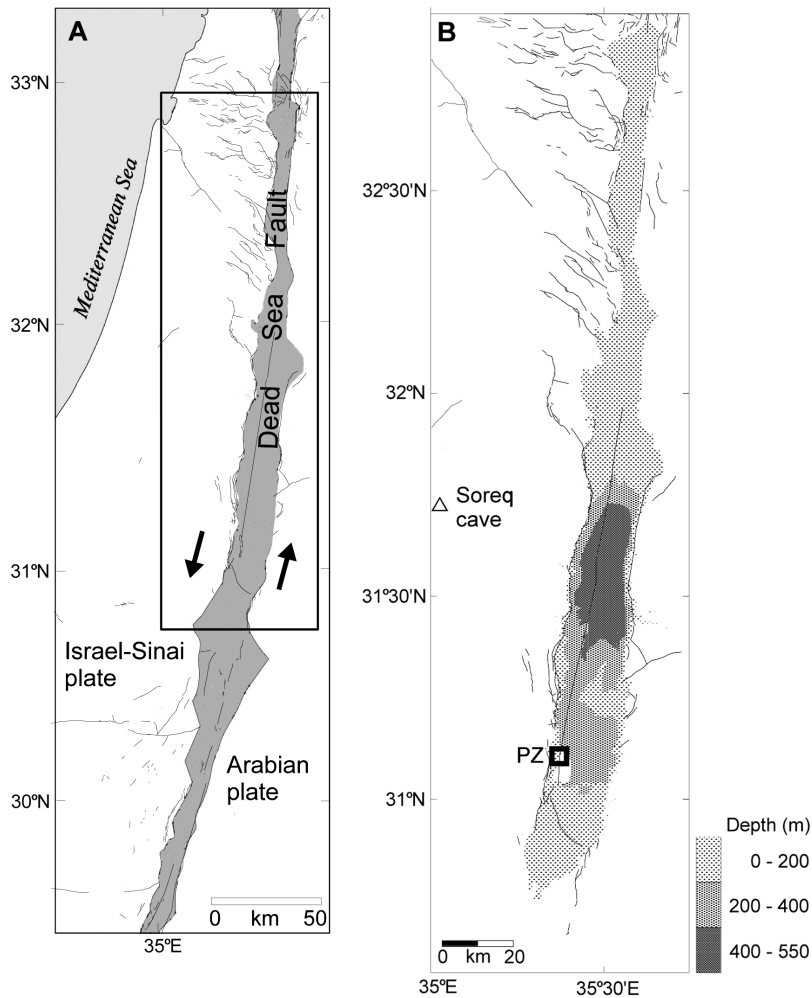


**Figure 1. A:** Location map showing potentially active faults along Dead Sea transform (Bartov et al., 2002). Shaded area denotes Dead Sea rift valley. Arrows mark sense of relative plate movement along transform. Box marks extent of B.

**B:** Potentially active faults along Dead Sea rift and depth of Lake Lisan for water level of 180 m below sea level, at which lake stood at 26–24 ka. For most of time between 70 and 28 ka lake stood at level of 280 m below sea level. Square marked PZ denotes location of PZ1 and PZ2 sections. Soreq Cave (triangle) includes damaged deposits that indicate strong earthquakes in Dead Sea rift (Kagan et al., 2005).

**Figure 2.** Thickness and occurrence in time of brecciated beds in PZ1 section. Symbols above vertical bars denote lithology overlying brecciated beds. Circles—beds of laminated gypsum and detritus (forming BGD couplets); triangles—detritus beds (forming BD couplets); diamonds—laminated aragonite and detritus, representing normal lake sedimentation. Gray rectangle marks sedimentation hiatus at PZ1. Horizontal lines show ages of seismites at Soreq Cave (Fig. 1). Broken line (ca. 13.5 ka) denotes minimum age of collapsed ceiling in nearby Har Tuv Cave (Kagan et al., 2005) and may be matched to  $15.9 \pm 0.8$  ka BGD couplet.

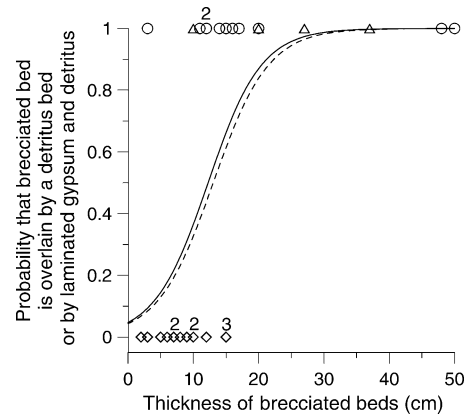
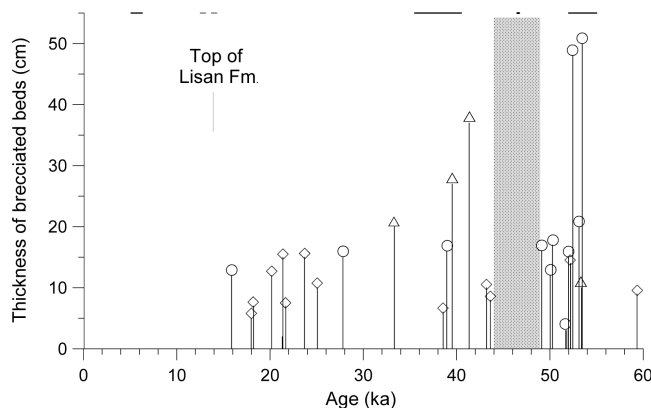


**Figure 3.** Logistic function showing that thicker brecciated beds in PZ1 section have higher probability to be overlain by beds of laminated gypsum and detritus (forming BGD couplets, circles) and by detritus beds (forming BD couplets, triangles) rather than by beds of laminated aragonite and detritus (forming BD couplets, diamonds). Numbers above symbols denote number of beds with identical thickness. Full line is for both BGD and BD couplets ( $p = 0.02$ , where  $p$  denotes p-value obtained in testing null hypothesis that layering is random) and broken line is for BGD couplets only ( $p = 0.05$ ). Since  $p \leq 0.05$  we reject null hypothesis that layering pattern is not related to thickness of brecciated beds.

mis running up and down beaches, is well known (Scheffers and Kelletat, 2003).

Could tsunamis and seiches have been formed in Lake Lisan by faulting? The generation of 10 m tsunami waves from faulting was numerically simulated for  $35 \times 19$  km, 500-m-deep Lake Tahoe (California-Nevada, United States) (Ichinose et al., 2000). Tsunami occurrence in the  $50 \times 15$  km, 300-m-deep Dead Sea is reported for several historic earthquakes (Amiran et al., 1994) that probably originated on faults within the Dead Sea pull-apart (Ken-Tor et al., 2001; Niemi and Ben-Avraham, 1994; Shapira et al., 1993; Reches and Hoexter, 1981; Marco et al., 2003).

Simulations of a tsunami for Lake Lisan at a water level of  $-280$  m (maximum depth of 450 m; Fig. 1B) that prevailed during most of Lake Lisan history (Bartov et al., 2003) were carried out with  $M_w$  7.3 earthquakes associated with left-lateral strike-slip faults having a rake of  $-30^\circ$  and a peak dip-slip component of 2.7 m. This is in accord with fault-plane solutions for earthquakes along the Dead Sea transform, reflecting the transtensional nature of its basins (Salamon et al., 2003; Shamir et al., 2003; Lubberts and Ben-Avraham, 2002). The simulations resulted in waves as high as 6–8 m, lasting for  $\sim 2$  h. A decrease of  $M_w$  to 6.9 and 6.6, and the peak dip-slip component to 1.5 m and 1.1 m, respectively, resulted in maximum wave heights of 3–5 m and 2–3 m, respectively (Ichinose and Begin, 2004).

These results were obtained for a fault whose main slip reached the surface within the deep basin of the lake, which is also the present deep basin of the Dead Sea (Fig. 1). On the other hand, for a fault of similar characteristics whose main dip slip is located in the northern, shallower basin of Lake Lisan, the tsunami simulation resulted in a maximum wave height of only 2 m (Ichinose and Begin, 2004).

## DISCUSSION

In following these results, we assume that (1) earthquakes with magnitudes of  $M > 7$  were capable of generating high seiches in Lake Lisan, which could have caused mixing of the water column, formation of gypsum, and deposition of gypsum above brecciated beds, thus forming BGD couplets; and (2) the occurrence of a Lisan BGD couplet constrains the location of the activated fault that caused the earthquakes to the area near the deep basin of Lake Lisan, <100 km north of the PZ sections (Fig. 1).

Building on these special circumstances, we examine the time series of the 11 BGD couplets in the PZ1 section, assuming that they represent  $M > 7$  earthquakes in the Dead Sea basin. For each BGD couplet we estimated the age of the top of the brecciated beds, according to their height above the bottom of the PZ1 section (Haase-Schramm et al., 2004; Table DRA [see footnote 1]). With these ages, we calculated for each BGD couplet the time that elapsed since the occurrence of the previous one (Fig. 4), and it can be seen that, following the cluster of strong earthquakes at 53.5–49 ka, there is an increase in the interval between strong earthquakes.

An independent proxy of strong earthquakes in the Dead Sea rift, inferred from damaged deposits at the Soreq Cave, 40 km west of the Dead Sea (Fig. 1) (Kagan et al., 2005), conforms to the logarithmic fit of the BGD couplets (Figs. 2 and 4). Its extrapolation to the Holocene is also supported by a 1.6 m vertical slip on the western border fault of the Dead Sea, dated as  $4.6 \pm 0.9$  ka (Gluck, 2002). Summarizing, since ca. 40 ka, the recurrence interval of strong earthquakes in the Dead Sea basin has been 7.5–12 k.y. (Fig. 4).

We now compare this paleoseismic record with the present seismicity in the Dead Sea area. Its magnitude-frequency relationship for  $M_L \leq 6.2$  earthquakes, augmented by a historic record that is assumed to be complete for  $M \geq 6$  since A.D. 1000, was described as:

$$N = \alpha \{ \exp[-\beta(M - M_{\min})] - \exp[-\beta(M_{\max} - M_{\min})] \} \div \{ 1 - \exp[-\beta(M_{\max} - M_{\min})] \}, \quad (1)$$

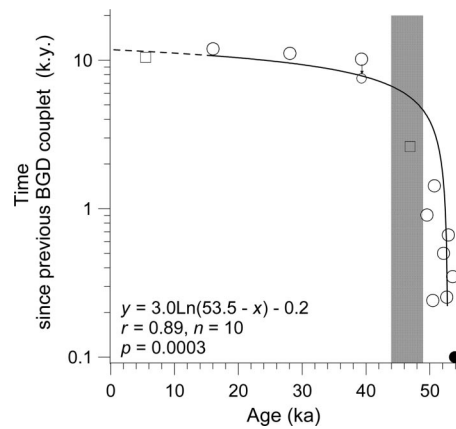


**Figure 4.** Time interval to previous BGD couplet (brecciated beds overlain by beds of laminated gypsum and detritus) in PZ1 section (circles; solid circle marks first BGD couplet, at 53.5 ka) as function of time. BGD couplets are assumed to represent  $M > 7$  earthquakes that occurred <100 km north of PZ1. After 39 ka, recurrence interval is ~11 k.y. Squares—data from Soreq Cave seismites (Kagan et al., 2005) (Fig. 1). Data-point shift occurs (small circle) if Soreq Cave seimite at 46.5 ka is included in calculations of time intervals. Gray rectangle marks hiatus in sedimentation at PZ1. Logarithmic fit was calculated on basis of BGD couplets alone and was extrapolated to present (broken line);  $p$  is  $p$ -value for testing hypothesis that correlation coefficient  $r$  results from random set of data points. Logarithmic fit may indicate fault healing.

where  $N$  is the annual frequency of earthquakes of magnitude  $M$  or greater;  $M_{\min}$  (the minimum magnitude considered) = 4;  $M_{\max}$  (the maximum probable magnitude) = 7.5;  $\alpha = 0.289$ ; and  $\beta = 2.21$  (Shapira and Hofstetter, 2002). Extrapolation of this formula to  $M > 6.5$  (Fig. 5) shows that a recurrence interval of 7.5–12 k.y., as deduced from the record of BGD couplets for strong earthquakes in the period 39–5.1 ka, conforms to earthquakes with magnitude 7.2–7.3 (assuming  $M_{\max} = 7.5$ ). After testing the sensitivity of this result to different values of the maximum probable magnitude ( $7.4 < M_{\max} < 7.7$ ) in the Dead Sea basin, such a recurrence interval conforms to earthquakes with magnitude 7.1–7.4 (Fig. 5). These estimates of earthquake magnitude are similar to the magnitude that was shown previously to be capable of generating high seiches in Lake Lisan and that probably caused mixing of the lake water column and the formation of BGD couplets in the Lisan Formation. This similarity in magnitudes suggests that the present seismic regime in the Dead Sea area has been stationary since ca. 40 ka.

The meagerness of strong earthquakes in this record indicates a deficiency in seismic moment relative to the  $>5$  mm/yr slip rate based on the geological evidence and to the

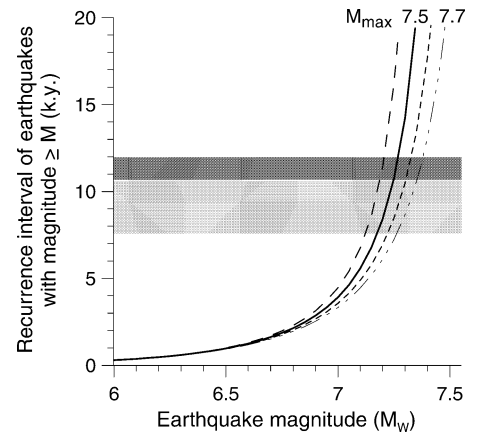


**Figure 5.** Recurrence interval (k.y.) for strong earthquakes in Dead Sea basin extrapolated from current seismicity (relationship 1 in text; Shapira and Hofstetter, 2002). Numbers are different values assumed for maximum probable magnitude ( $M_{\max}$ ) in Dead Sea basin. Gray rectangle shows range of recurrence intervals for strong earthquakes for period 39–5.1 ka, based on age of brecciated beds overlain by beds of laminated gypsum and detritus and seismites at Soreq Cave (Fig. 4); darker shaded rectangle is for period 28–5.1 ka. These recurrence intervals are shown here to characterize earthquake magnitudes of 7.1–7.4. Digital simulations showed that earthquakes in Dead Sea basin within this range of magnitudes were capable of generating BGD couplets. We conclude from these observations that present seismic regime in Dead Sea basin has been stationary for past 40 k.y.

$3.3 \pm 0.4$  mm/yr based on global positioning system measurements (Wdowinski et al., 2004). Since such moment deficiency characterizes the Dead Sea Fault in the past 100 yr of measured seismicity (Salamon et al., 2003), as well as in the k.y. record of its historic seismicity (Ben Menahem, 1981; Garfunkel et al., 1981), the seismic regimes at present and for the past 40 k.y. are also similar in this respect.

The antiquity of a present seismic regime has not been discussed in previous studies, probably because of lack of an adequate data set. The series of BGD couplets, as extracted from Lake Lisan seismites and partially supported by cave seismites, provides a unique example of a well dated, long, and 85% complete prehistoric seismic record. The 40 k.y. stability of the seismic regime indicates the time constant for the model of earthquake mode switching (Ben-Zion et al., 1999; Lyakhovskiy et al., 2001), which predicts a gradual passage from a clustering of strong earthquakes to a quiet period.

Since the deduced strong earthquakes are spatially well constrained, this series may afford an opportunity to examine long-term fault relaxation. The time-logarithmic fit implies healing of the fault system, as it is similar to

both the logarithmic increase of the static friction coefficient as derived in the laboratory (Marone, 1998) and the logarithmic decrease with time of damage along a fault (healing) as derived from damage theory (Lyakhovsky et al., 2001). If so, a source for such change may be a diminishing strain rate after the first strong earthquake in the sequence, as can be expected from viscoelastic relaxation below the brittle upper crust, because the strain rate in the lower crust (and loading rate in the upper crust) would decrease with time after the largest event. Hence, the time interval it takes to accumulate a certain fixed value of slip deficit would gradually increase (Ben-Zion et al., 1993).

#### ACKNOWLEDGMENTS

We gratefully acknowledge the helpful suggestions of A. Agnon, G. Baer, S. Frydman, Z. Gvirtzman, O. Katz, R. Bookman, Y. Mimran, A. Salamon, A. Shapira, and M. Stein, as well as *Geology* reviewers S. Wdowinski and an anonymous reviewer. We thank Y. Ben Zion and V. Lyakhovsky for fruitful discussions. The simulation of tsunamis in the Dead Sea and Lake Lisan was supported by the Israel Committee for Earthquake Readiness. We thank J.K. Hall for providing the digital terrain model that served as a basis for the tsunami simulations.

#### REFERENCES CITED

- Amiran, D.H.K., Arieh, E., and Turcotte, T., 1994, Earthquakes in Israel and adjacent areas: Macroseismic observations since 100 B.C.E.: *Israel Exploration Journal*, v. 44, p. 260–305.
- Bartov, Y., Sneh, A., Fleischer, L., Arad, V., and Rosensaft, M., 2002, Potentially active faults in Israel: Geological Survey of Israel Report GSI/29/2002, p. 8.
- Bartov, Y., Goldstein, S.L., Stein, M., and Enzel, Y., 2003, Catastrophic arid episodes in the eastern Mediterranean linked with the North Atlantic Heinrich events: *Geology*, v. 31, p. 439–442, doi: 10.1130/0091-7613(2003)031.0.CO;2.
- Ben Menahem, A., 1981, Variation of slip and creep along the Levant Rift over the past 4500 years: *Tectonophysics*, v. 80, p. 183–197.
- Ben-Zion, Y., Rice, J.R., and Dmowska, R., 1993, Interaction of the San Andreas fault creeping segment with adjacent great rupture zones and earthquake recurrence at Parkfield: *Journal of Geophysical Research*, v. 98, p. 2135–2144.
- Ben-Zion, Y., Dahmen, K., Lyakhovsky, V., Ertas, D., and Agnon, A., 1999, Self-driven mode switching of earthquake activity on a fault system: *Earth and Planetary Science Letters*, v. 172, p. 11–21.
- Garfunkel, Z., 1981, Internal structure of the Dead Sea leaky transform (rift) in relation to plate kinematics: *Tectonophysics*, v. 80, p. 81–108, doi: 10.1016/0040-1951(81)90143-8.
- Garfunkel, Z., Zak, Y., and Freund, R., 1981, Active faulting in the Dead Sea rift: *Tectonophysics*, v. 80, p. 1–26, doi: 10.1016/0040-1951(81)90139-6.
- Gluck, D., 2002, The landscape evolution of the southwestern Dead Sea basin and the paleoseismic record of the southwestern marginal fault of the Dead Sea basin and of the Carmel fault during the late Pleistocene and Holocene: Geological Survey of Israel Report GSI/4/02, 86 p. (in Hebrew, with English abstract).
- Haase-Schramm, A., Goldstein, S.L., and Stein, M., 2004, U-Th dating of Lake Lisan aragonite (late Pleistocene Dead Sea) and implications for glacial East Mediterranean climate change: *Geochimica et Cosmochimica Acta*, v. 68, p. 985–1005, doi: 10.1016/j.gca.2003.07.016.
- Ichinose, G.A., and Begin, Z.B., 2004, Simulation of tsunamis and lake seiches for late Pleistocene Lake Lisan and for the Dead Sea: Geological Survey of Israel Report GSI/7/2004, 64 p.
- Ichinose, G.A., Satake, K., Anderson, J.G., Schweickert, R.A., and Lahran, M.M., 2000, The potential hazard from tsunami and seiche waves generated by large earthquakes within Lake Tahoe, California-Nevada: *Geophysical Research Letters*, v. 27, p. 1203–1206, doi: 10.1029/1999GL011119.
- Kagan, E.J., Agnon, A., Bar-Matthews, M., and Ayalon, A., 2005, Dating large infrequent earthquakes by damaged cave deposits: *Geology*, v. 33, p. 261–264.
- Ken-Tor, R., Agnon, A., Enzel, Y., Stein, M., Marco, S., and Negen-dank, J.F.W., 2001, High-resolution geological record of historic earthquakes in the Dead Sea basin: *Journal of Geophysical Research*, v. 106, p. 2221–2234, doi: 10.1029/2000JB900313.
- Lubberts, R.K., and Ben-Avraham, Z., 2002, Tectonic evolution of the Qumran basin from high-resolution 3.5-kHz seismic profiles and its implication for the evolution of the northern Dead Sea basin: *Tectonophysics*, v. 346, p. 91–113.
- Lyakhovsky, V., Ben-Zion, Y., and Agnon, A., 2001, Earthquake cycle, fault zones, and seismicity patterns in a rheologically layered lithosphere: *Journal of Geophysical Research*, v. 106, p. 4103–4120, doi: 10.1029/2000JB900218.
- Machlus, M., Enzel, Y., Goldstein, S.L., Marco, S., and Stein, M., 2000, Reconstructing low levels of Lake Lisan by correlating fan-delta and lacustrine deposits: *Quaternary International*, v. 73–74, p. 137–144, doi: 10.1016/S1040-6182(00)00070-7.
- Marco, S., 1996, Paleomagnetism and paleoseismology in the late Pleistocene Dead Sea graben [Ph.D. thesis]: Hebrew University of Jerusalem, 95 p.
- Marco, S., and Agnon, A., 1995, Prehistoric earthquake deformations near Masada, Dead Sea graben: *Geology*, v. 23, p. 695–698, doi: 10.1130/0091-7613(1995)023.0.CO;2.
- Marco, S., Stein, M., Agnon, A., and Ron, H., 1996, Long-term earthquake clustering: A 50,000-year paleoseismic record in the Dead Sea Graben: *Journal of Geophysical Research*, v. 101, p. 6179–6191, doi: 10.1029/95JB01587.
- Marco, S., Hartal, M., Hazan, N., Lev, L., and Stein, M., 2003, Archaeology, history, and geology of the A.D. 749 earthquake, Dead Sea transform: *Geology*, v. 31, p. 665–668, doi: 10.1130/G19516.1.
- Marone, C., 1998, Laboratory-derived friction laws and their application to seismic faulting: *Annual Review of Earth and Planetary Science*, v. 26, p. 643–696, doi: 10.1146/annurev.earth.26.1.643.
- Migowski, C., Agnon, A., Bookman, R., Negen-dank, J.F.W., and Stein, M., 2004, Recurrence pattern of Holocene earthquakes along the Dead Sea Transform revealed by varve-counting and radiocarbon dating of lacustrine sediments: *Earth and Planetary Science Letters*, v. 222, p. 301–314.
- Niemi, T.M., and Ben-Avraham, Z., 1994, Evidence for Jericho earthquakes from slumped sediments of the Jordan River delta in the Dead Sea: *Geology*, v. 22, p. 395–398, doi: 10.1130/0091-7613(1994)022.3.CO;2.
- Reches, Z., and Hoexter, D.F., 1981, Holocene seismic and tectonic activity in the Dead Sea area: *Tectonophysics*, v. 80, p. 235–254, doi: 10.1016/0040-1951(81)90151-7.
- Salamon, A., Hofstetter, A., Garfunkel, Z., and Ron, H., 2003, Seismotectonics of the Sinai subplate—The eastern Mediterranean region: *Geophysical Journal International*, v. 155, p. 149–173, doi: 10.1046/j.1365-246X.2003.02017.x.
- Scheffers, A., and Kelletat, D., 2003, Sedimentologic and geomorphologic tsunami imprints worldwide—A review: *Earth-Science Reviews*, v. 63, p. 83–92.
- Schramm, A., Stein, M., and Goldstein, S.L., 2000, Calibration of the  $^{14}\text{C}$  time scale to >40 ka by  $^{234}\text{U}$ - $^{230}\text{Th}$  dating of Lake Lisan sediments (last glacial Dead Sea): *Earth and Planetary Science Letters*, v. 175, p. 27–40, doi: 10.1016/S0012-821X(99)00279-4.
- Seed, H., and Idriss, I.M., 1982, Ground motions and soil liquefaction during earthquakes: Oakland, California, *Earthquake Engineering Research Institute*, 134.
- Shamir, G., Baer, G., and Hofstetter, A., 2003, Three-dimensional elastic earthquake modeling based on integrated seismological and InSAR data: The  $M_w = 7.2$  Nuweiba earthquake, Gulf of Elat/Aqaba 1995 November: *Geophysical Journal International*, v. 154, p. 731–744.
- Shapira, A., and Hofstetter, A., 2002, Seismic parameters of seismogenic zones. Appendix C, in Shapira, A., 2002, An updated map of peak ground accelerations for the Israel Standard 413: Israel Geophysical Institute Report 592/230/02 74 p. (in Hebrew, with appendices in English).
- Shapira, A., Avni, R., and Nur, A., 1993, New estimate of the Jericho earthquake epicenter of July 11, 1927: *Israel Journal of Earth Sciences*, v. 42, p. 93–96.
- Stein, M., Starinsky, A., Katz, A., Goldstein, S.L., Machlus, M., and Schramm, A., 1997, Strontium isotopic, chemical, and sedimentological evidence for the evolution of Lake Lisan and the Dead Sea: *Geochimica et Cosmochimica Acta*, v. 61, p. 3975–3992, doi: 10.1016/S0016-7037(97)00191-9.
- Wdowinski, S., Bock, Y., Baer, G., Prawirodirdjo, L., Bechor, N., Naman, S., Knafo, R., Forrai, Y., and Melzer, Y., 2004, GPS measurements of current crustal movements along the Dead Sea fault: *Journal of Geophysical Research*, v. 109, B05403 p. 1–16.
- Youd, T.L., and Perkins, D.M., 1987, Mapping of liquefaction severity index: *Journal of Geotechnical Engineering*, v. 113, p. 1374–1392.

Manuscript received 17 August 2004

Revised manuscript received 22 December 2004

Manuscript accepted 23 December 2004

Printed in USA

DR2005045

Begin

## Data Repository Items

**Table DRA: Data on brecciated beds in the PZ1 and PZ2 sections**

A- alternating laminae of aragonite and detritus. G- alternating laminae of gypsum and detritus. D- detritus bed. D-G- detritus bed overlain by a G-bed. Age assignments are for PZ1. Matching of brecciated beds in the two sections is tentative.

Age, (ka)*	PZ1					PZ2				
	No	Height of top (cm)	Lithology		Thick -ness (cm)	No	Height of top (cm)	Lithology		Thick -ness (cm)
			Above	Below				Above	Below	
						<b>34</b>	3701	A	A	3
						<b>33</b>	3686	A	A	3
						<b>32</b>	3663	A	A	6
						<b>31</b>	3557	A	A	3
15.9	<b>29</b>	3762	G	A	12	<b>30</b>	3507	D	A	18
18.0	<b>28</b>	3612	A	A	5	<b>29</b>	3483	D	A	6
						<b>28</b>	3468	D	A	5
18.2	<b>27</b>	3594	A	A	7	<b>27</b>	3442	G	A	5
20.2	<b>26</b>	3455	A	A	12	<b>26</b>	3359	A	A	9
21.3	<b>25</b>	3374	A	A	2	<b>25</b>	3344	A	A	10
21.4	<b>24</b>	3369	A	A	15	<b>24</b>	3297	A	A	3
21.7	<b>23</b>	3347	A	A	7	<b>23</b>	3276	A	A	6
23.7	<b>22</b>	3204	A	A	15	<b>22</b>	3223	A	A	3
25.1	<b>21</b>	3105	A	A	10	<b>21</b>	3020	A	A	3
27.8	<b>20</b>	2909	G	A	15	<b>20</b>	3008	D	A	2
33.3	<b>19</b>	2515	D	A	20	<b>19</b>	2979	D	A	4
38.6	<b>18</b>	2142	A	A	6	<b>18</b>	2899	A	A	4
38.9	<b>17</b>	2114	G	D	16	<b>17</b>	2689	D	A	31
						<b>16</b>	2627	A	A	3
39.5	<b>16</b>	2073	D-G	A	27	<b>15</b>	2588	D	A	33
41.3	<b>15</b>	1943	D-G	A	37	<b>14</b>	2499	D-G	A	45
43.2	<b>14</b>	1810	A	D	10					
43.6	<b>13</b>	1781	A	G	8					
49.1	<b>12</b>	1745	G	A	16	<b>13</b>	2255	D-G	A	7
50.0	<b>11</b>	1602	G	A	12	<b>12</b>	2115	A	A	5
50.3	<b>10</b>	1564	G	A	17	<b>11</b>	1726	D	A	5
51.7	<b>9</b>	1339	G	A	3	<b>10</b>	1627	D	A	10
51.8	<b>8</b>	1320	A	A	3	<b>9</b>	1354	A	A	13
52.0	<b>7</b>	1294	A	D	15	<b>8</b>	1321	A	A	16
52.2	<b>6</b>	1260	G	A	14	<b>7</b>	1147	D	A	19
52.4	<b>5</b>	1220	G	A	48	<b>6</b>	1089	D	A	14
53.1	<b>4</b>	1115	G	G	20	<b>5</b>	1052	D	A	3
						<b>4</b>	1018	A	D	6
53.4	<b>3</b>	1074	D-G	G	10	<b>3</b>	955	D	D	20
53.5	<b>2</b>	1060	G	G	50	<b>2</b>	896	D	A	30
59.3	<b>1</b>	134	A	A	9	<b>1</b>	405	A	A	5

\*The age (T, ka) of the top of the brecciated beds was estimated according to their height (H, m) above the bottom of the PZ1 section according to the following regressions (Haase-Schrammet al., 2004):  $T=68.5-1.4H$  for  $0.8<H<17.7$  and  $T=60.2-0.63H$  for  $17.7<H<38.5$ .

Begin

## Table DRB

TABLE DRB. LITHOLOGY OF BEDS BELOW AND ABOVE  
THE 34 BRECCIATED BEDS IN THE PZ2 SECTION

	Lithology		Total
	Gypsum* or detritus	Aragonite†	
<u>Position of beds relative to brecciated beds</u>			
Above	17 <sup>§</sup> (9.5)	17 (24.5)	34
Below	2 <sup>#</sup> (9.5)	32 (24.5)	34
Total	19	49	68

*Note:* Numbers in parentheses are expected values if there is no connection between lithology and position relative to the brecciated beds. Probability of random occurrence:  $p = .0002$  (Yates correction applied to the  $\chi^2$  test).

\* Alternating laminae of gypsum and detritus.

† Alternating laminae of aragonite and silt.

§ 1 gypsum bed.

#2 detritus beds.

Begin

## Table DRC

TABLE DRC. LITHOLOGY OF BEDS BELOW AND ABOVE  
THE 29 BRECCIATED BEDS IN THE PZ1 SECTION

	Lithology		Total
	Gypsum* or detritus	Aragonite†	
<u>Position of beds relative to brecciated beds</u>			
Above	15 <sup>§</sup> (11)	14 (18)	29
Below	7 <sup>#</sup> (9.5)	22 (18)	29
Total	22	36	58

*Note:* Numbers in parentheses are expected values if there is no connection between lithology and position relative to the brecciated beds. Probability of random occurrence:  $p = .058$  (Yates correction applied to the  $\chi^2$  test).

\* Alternating laminae of gypsum and detritus.

† Alternating laminae of aragonite and silt.

§ 4 detritus beds, of which 3 are overlain by alternating laminae of gypsum and detritus.

#3 detritus beds.

## Figure DRD

**Figure DRD.** Logistic function, showing that thicker brecciated beds in the PZ2 section have a higher probability to be overlain by detritus beds (BD couplets, triangles) and beds of laminated gypsum and detritus (BGD couplets, circles), rather than by beds of laminated aragonite and detritus (diamonds). Digits above symbols denote number of beds with identical thickness. Full line is for both BGD couplets (brecciated beds overlain by beds of laminated gypsum and detritus) and BD couplets (brecciated beds overlain by beds of detritus).  $p = 0.03$ , where  $p$  denotes the p-value obtained in testing the null hypothesis that the layering is random. Since  $p \leq 0.05$  we reject the null hypothesis that the layering pattern is not related to the thickness of the brecciated beds.

